JOC Article

Diastereospecific Photocyclization of a Isopropylbenzophenone Derivative in Crystals and the Morphological Changes

Hideko Koshima,*,† Michitaro Fukano,† and Hidehiro Uekusa‡

Department of Materials Science and Biotechnology, Ehime University, Matsuyama 790-8577, Japan, and Department of Chemistry and Materials Science, Tokyo Institute of Technology, O-Okayama, Meguro-ku, Tokyo 152-8551, Japan

koshima@eng.ehime-u.ac.jp

Received May 12, 2007

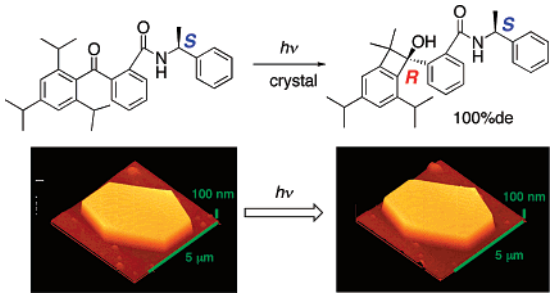

Reaction of crystals of 2,4,6-triisopropylbenzophenone derivative with the (*S*)-phenylethylamide group caused diastereospecific Norrish type II photocyclization by UV irradiation to give (*R*,*S*)-cyclobutenol as a sole product. In contrast, the solution photolysis gave an almost 1:1 mixture of (*R*,*S*)- and (*S*,*S*)-cyclobutenol. The specific diastereodifferentiation in the crystalline state is attributed to the smooth transformation with minimum molecular motion due to the very similar molecular shapes as well as the 2-fold helical arrangements between the reactant crystal and the product (*R*,*S*)-cyclobutenol crystal. UV irradiation of the bulk crystals led to cracking and breaking into small fragments. In contrast, the microcrystals maintained the single-crystalline morphology in the course of photocyclization, suggesting the single-crystal-to-single-crystal transformation.

Introduction

Since the study of [2 + 2] photocyclization of *trans*-cinnamic acids in 1964,[1] a large number of crystalline-state reactions have been reported.[2−6] The relationship between the crystal structures and the reactions has been elucidated so far. In contrast, the morphological changes on the crystals by the reactions have been scarcely studied. It was reported that the topochemical photopolymerization of diolefin crystals gave rise to cracks and deformation.[7] Atomic force microscopic (AFM) study made possible the observation that the photodimerizations of *trans*-cinnamic acids and anthracenes in the crystalline state induced surface morphological changes at tens and hundreds of nanometers level by the transportation and rebuilding of the surface molecules.[8] Surface relief gating (SRG) formation was demonstrated on the single crystal of 4-(dimethylamino)azobenzene by repeated irradiation with two coherent laser beams.[9] Reversible shape changes were also reported on a photochromic diarylethene single crystal by UV irradiation.[10]

* To whom correspondence should be addressed.
† Ehime University.
‡ Tokyo Institute of Technology.

(1) Cohen, M. D.; Schmidt, G. M. *J. Chem. Soc.* **1964**, 1996−2000.
(2) *Organic Solid State Chemistry*; Desiraju, G. R., Ed.; Elsevier: New York, 1987.
(3) *Reactivity in Molecular Crystals*; Ohashi, Y., Ed.; Kodansha-VCH: Tokyo, 1993.
(4) Tanaka, K.; Toda, F. *Chem. Rev.* **2000**, *100*, 1025−1074.
(5) *Organic Solid-State Reactions*; Toda, F., Ed.; Kluwer Academic Publishers: Dordrecht, 2002.
(6) *Chiral Photochemistry*; Inoue, Y., Ramamurthy, V., Eds.; Marcel Dekker, Inc.: New York, 2004.
(7) (a) Nakanishi, H.; Hasegawa, M.; Sasada, Y. *J. Polym. Sci. Polym. Chem. Ed.* **1972**, *10*, 1537−1553. (b) Nakanishi, H.; Hasegawa, M.; Kirihara, H.; Yurugi, T. *Nippon Kagaku Zasshi* **1977**, 1046−1050. (c) Hasegawa, M. *Chem. Rev.* **1983**, *83*, 507−518.
(8) (a) Kaupp, G. *Angew. Chem., Int. Ed. Engl.* **1992**, *31*, 592−595. (b) Kaupp, G. *Angew. Chem., Int. Ed. Engl.* **1992**, *31*, 595−598. (c) Kaupp, G.; Plagmann, M. *J. Photochem. Photobiol. A: Chem.* **1994**, *80*, 399−407.
(9) Nakano, H.; Tanino, T.; Shirota, Y. *Appl, Phys. Lett.* **2005**, *87*, 061910.

10.1021/jo071005i CCC: $37.00
Published on Web 08/10/2007

SCHEME 1

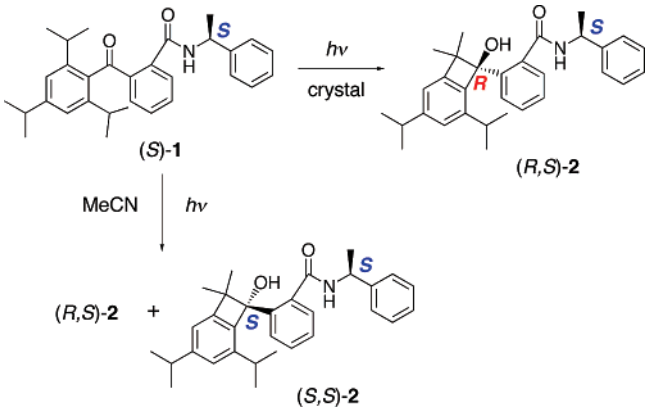

It is known that 2,4,6-triisopropylbenzophenone derivatives undergo Norrish type II photocyclization to give the cyclobutenol in the solid state and in the solution phase.[11] In our previous papers, it was revealed that the highly enantioselective photocyclization of the carboxylic acid derivatives was achieved in the salt crystals with chiral and achiral amines, and the reactions proceeded via single-crystal-to-single-crystal transformation.[12−14] Herein, we report the diastereospecific photocyclization of 2-(2,4,6-triisopropybenzoyl)((*S*)-1-phenylethyl)benzamide (*S*)-**1** in the crystalline state and the morphological changes of single crystals.

Results and Discussion

UV irradiation of the pulverized crystals of (*S*)-**1** with a 400 W high-pressure mercury lamp through Pyrex glass under argon at 20 °C for 8 h caused photocyclization to afford *R*-cyclobutenol (*R*,*S*)-**2** as the sole product in 100% chemical yield and 100% de (Scheme 1). No diastereomer (*S*,*S*)-**2** was obtained by silica gel column chromatography or detected by HPLC analysis, confirming the diastereospecific photocyclization in the crystalline state. In contrast, the solution photolysis of (*S*)-**1** in acetonitrile gave a mixture of (*R*,*S*)-**2** and (*S*,*S*)-**2** in 24% and 21% chemical yield, respectively, revealing the low diastereoselectivity of only 6% de.

We carried out the X-ray crystallographic analyses of the reactant as well as the products in order to elucidate the mechanism for the diastereospecific photocyclization in the crystal (*S*)-**1**. The single crystals of (*R*,*S*)-**2** and (*S*,*S*)-**2** were prepared by slow evaporation of the acetonitrile solutions. The absolute structures were determined on the basis of the *S* configuration of phenylethylamide group of the molecules. The selected crystal data are summarized in Table 1.

ORTEP drawings of the reactant (*S*)-**1** and the products (*R*,*S*)-**2** and (*S*,*S*)-**2** are shown in Figure 1a,d,g, respectively.

TABLE 1. Selected Crystal Data

	(*S*)-**1**	(*R*, *S*)-**2**	(*S*, *S*)-**2**
crystal system	orthorhombic	monoclinic	tetragonal
space group	$P2_12_12_1$ (#19)	$P2_1$ (#4)	$P4_1$(#76)
a, Å	21.341(2)	10.119(2)	11.1250(8)
b, Å	9.6458(7)	9.494(1)	11.1250(8)
c, Å	13.273(1)	14.032(2)	22.9386(19)
β, deg	90.0	97.056(8)	90.0
V, Å^3	2732.2(4)	1337.8(3)	2839.0(4)
Z	4	2	4
D, g cm^{-3}	1.108	1.131	1.066

The molecular conformation of (*S*)-**1** is very similar to that of (*R*,*S*)-**2** but different from that of (*S*,*S*)-**2**. In the crystal (*S*)-**1**, a 2-fold helical chain is formed among the amide groups through the N−H---O═C hydrogen bond (2.17 Å) along the *b* axis (Figure 1b). The helical chains are alternatively arranged in opposite directions and a half translation along the *c*-axis (Figure 1c).

In the product crystal (*R*,*S*)-**2**, a 2-fold helical chain similar to that of (*S*)-**1** is formed among the amide groups through the N−H---O═C hydrogen bond (2.35 Å) along the *b* axis (Figure 1e). An intramolecular O−H---O═C hydrogen bond (1.61 Å) is also formed between the hydroxyl group and the carbonyl group. The helical chains are arranged in a direction along the *b* axis (Figure 1f). Despite the fact that the crystals (*S*)-**1** and (*R*,*S*)-**2** belong to different crystal systems, orthorhombic and monoclinic, respectively, the lengths of the *b* and *c* axes of the unit cell are very similar and the length of the *a* axis of (*R*,*S*)-**2** is almost half of that of (*S*)-**1** (Table 1). Therefore, the cell volume of (*R*,*S*)-**2** is almost half of that of (*S*)-**1**.

In contrast, the crystal system of (*S*,*S*)-**2** is cubic. A 4-fold helical chain in the clockwise direction is formed between the hydroxyl group and the amide group through the intermolecular H−O---H−N hydrogen bond (2.05 Å) along the *c* axis (Figures 1h and 1i). Intramolecular O−H---O═C hydrogen bond (1.64 Å) is also formed between the hydroxyl group and the carbonyl group. Thus, the molecular arrangement is different from those of (*S*)-**1** and (*R*,*S*)-**2**.

Irradiation of the crystal (*S*)-**1** with high-pressure mercury lamp through Pyrex glass causes n,π^* excitation of the carbonyl O1 oxygen atom of the (*S*)-**1** molecule (Figure 1a). The excited O1 atom has the possibility of abstraction of both the methine H1 and H2 hydrogen atoms of two *o*-isopropyl groups to produce (*R*)- and (*S*)-ketyl radicals, respectively, and corresponding methine radicals. Then the radicals approach each other and finally couple to afford (*R*)- and (*S*)-cyclobutenol, i.e., both the diastereomeric products (*R*,*S*)-**2** (Figure 1d) and (*S*,*S*)-**2** (Figure 1g). However, only (*R*,*S*)-**2** was obtained by the crystalline-state photocyclization; (*S*,*S*)-**2** was not at all produced. Hence, we compared all the geometrical parameters for the two possible hydrogen atom abstractions formulated by Scheffer.[15] The both distances of O1---H1 (2.83 Å) and O1---H2 (2.97 Å) are enough short and similar to each other. The angles of C1−O1−H1 (57.3°) and C1−O1−H2 (53.7°) are similar. Furthermore, the angles defined as the degree to which the abstracted H1 and H2 hydrogen atoms lie outside the mean plane of the carbonyl group are similar: 53.7° and 52.9°, respectively. This means that the diastereospecific O1---H1 hydrogen abstraction could not be explained from the

(10) (a) Irie, M.; Kobatake, S.; Horichi, M. *Science* **2001**, *291*, 188−191. (b) Kobatake, S.; Takami, S.; Muto, H.; Ishikawa, T.; Irie, M. *Nature* **2007**, *446*, 778−781.

(11) (a) Ito, Y.; Nishimura, H.; Umehara, Y.; Yamada, Y.; Tone, M.; Matsuura, T. *J. Am. Chem. Soc.* **1983**, *105*, 1590−1597. (b) Ito, Y.; Matsuura, T. *Tetrahedron Lett.* **1988**, *29*, 3087−3090.

(12) (a) Koshima, H.; Maeda, A.; Matsuura, T.; Hirotsu, K.; Okada, K.; Mizutani, H.; Ito, Y.; Fu, T. Y.; Scheffer, J. R.; Trotter, J. *Tetrahedron: Asymmetry* **1994**, *5*, 1415−1418. (b) Hirotsu, K.; Okada, K.; Mizutani, H.; Koshima, H.; Matsuura, T. *Mol. Cryst. Liq. Cryst.* **1996**, *277*, 99−106.

(13) Koshima, H.; Matsushige, D.; Miyauchi, M. *CrystEngComm* **2001**, *33*, 1−3.

(14) Koshima, H.; Kawanishi, H.; Nagano, M.; Yu, H.; Shiro, M.; Hosoya, T.; Uekusa, H.; Ohashi, Y. *J. Org. Chem.* **2005**, *70*, 4490−4497.

(15) Scheffer, J. F. In *Organic Solid State Chemistry*; Desiraju, G. R., Ed.; Elsevier: New York, 1987; pp 1−45.

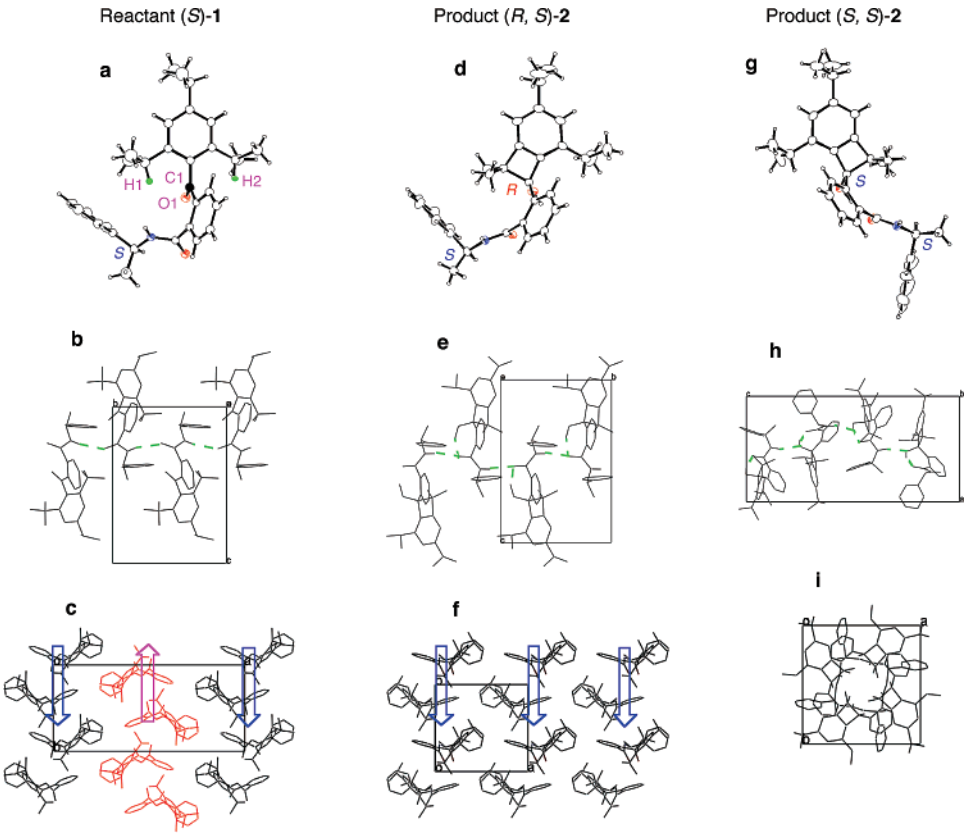

FIGURE 1. ORTEP drawings of (a) (*S*)-**1**, (d) (*R*,*S*)-**2**, and (g) (*S*,*S*)-**2**; the thermal ellipsoids are plotted at the 15% probability level. Molecular arrangements (b), (c) in (*S*)-**1**, (e), (f) in (*R*,*S*)-**2**, and (h), (i) in (*S*,*S*)-**2**; the hydrogen atoms are omitted for clarity. The green dotted lines in (b), (e), and (h) represent the hydrogen bonds.

geometrical parameters between the carbonyl oxygen atom and the two γ-hydrogen atoms.

Next, the diastereospecific photocyclization was discussed based on a cavity, which concept was introduced by Ohashi and co-workers.[16] The void space around the *o*-isopropyl groups and the phenone group of the reactant (*S*)-**1** is important because the moieties are accompanied with large motion by the hydrogen abstraction by the excited carbonyl oxygen. The surroundings are well represented by a cavity, which is defined as a space limited by a concave surface of the spheres of inter- and intramolecular atoms in the neighborhood. Figure 2 shows the stereoscopic drawings of cavities for the *o*-isopropyl groups and the phenone group of the reactant (*S*)-**1**. The cavities have the volumes of 66.3 (Figure 2a) and 59.0 Å^3 (Figure 2b), corresponding to produce (*R*,*S*)-**2** and (*S*,*S*)-**2**, respectively. The difference of cavities by 7.3 Å^3 is relatively large, and therefore, the formation of (*R*,*S*)-**2** in higher priority than (*S*,*S*)-**2** is reasonable. However, no formation of (*S*,*S*)-**2** cannot be explained from the smaller cavity size.

Recent intensive studies have revealed that crystalline state reactions proceed generally in the minimum molecular motion in the crystal lattice because the molecules are arranged at close positions in three-dimensional regularity and the motion is very restricted.[2−6] As shown in Figure 1a−f, the resemblance of molecular shapes and 2-fold helical arrangements in the crystals (*S*)-**1** and (*R*,*S*)-**2** suggests that the transformation from the molecule (*S*)-**1** to (*R*,*S*)-**2** can smoothly proceed within the helical chains by UV irradiation due to the minimum motion. In contrast, the molecular conformation and the 4-fold helical

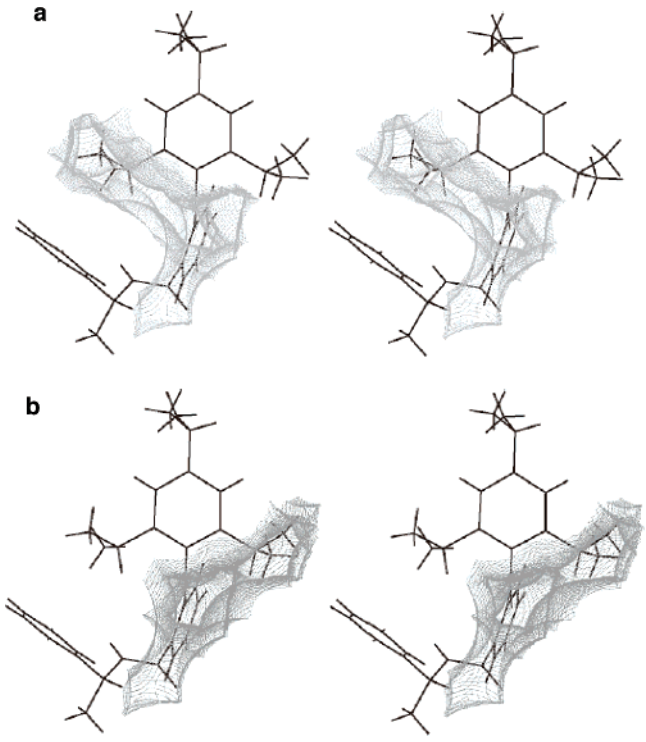

FIGURE 2. Stereoviews of the cavities for the *o*-isopropyl groups and the phenone group in the crystal (*S*)-**1**.

(16) Ohashi, Y.; Yanagi, K.; Kurihara, T.; Sasada, Y.; Ohgo, Y. *J. Am. Chem. Soc.* **1981**, *103*, 5805−5812.

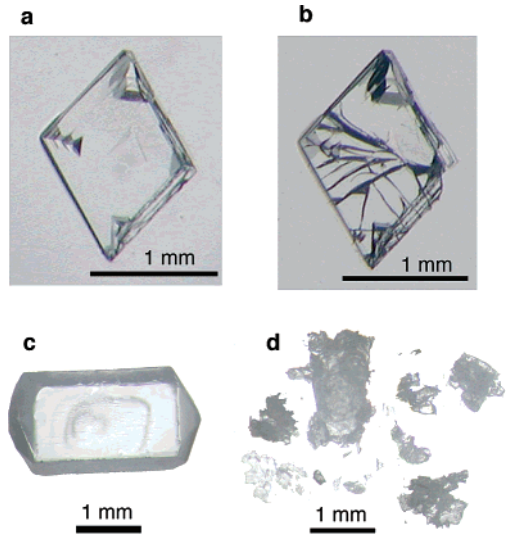

FIGURE 3. Morphology of bulk crystals of (*S*)-**1** before and after UV irradiation: crystals in (b) and (d) were obtained from the crystals in (a) and (c) after UV irradiation with a high-pressure mercury lamp under argon at 15 °C for 7 and 20 min, respectively.

arrangement in the crystal (*S*,*S*)-**2** (Figures 1g−i) are very different from those of (*S*)-**1** (Figure 1a−c). For the formation of (*S*,*S*)-2, the phenylethylamide group of molecule (*S*)-**1** must turn to the opposite side. As a matter of course, such the large motion within the restricted lattice is difficult. This is most probably the reason why (*S*,*S*)-**2** is not at all obtained as one of the diastereomeric products.

We observed the changes of surface morphology of the crystals of (*S*)-**1** during the photocyclization. UV irradiation of the bulk crystals led to cracking and finally breaking into small fragments (Figure 3). We understood the phenomenon unquestionably because the crystal structures of the reactant (*S*)-**1** and the product (*R*,*S*)-**2** were different, and therefore, the strain was accumulated to break the single crystals.

Next, the microcrystals of (*S*)-**1** were submitted to UV irradiation. The microcrystals were prepared by vaporizing the powder samples on a heater at slightly lower temperature than the melting point (142 °C), collecting the vapor on a quartz plate, and crystallizing at room temperature (Figure 5a). The photocyclization process was monitored by FT-IR spectroscopy. Figure 4a shows the change in the IR spectrum under UV irradiation. The intensities of the reactant (*S*)-**1** band at 1678 and 1640 cm^{-1} for the stretching vibration due to the benzophenone carbonyl group and the amide carbonyl group, respectively, decreased with an increasing UV irradiation time. Conversely, the intensity of the product (*R*,*S*)-**2** band at 1609 cm^{-1} for the stretching vibration due to the amide carbonyl group increased. Irradiation for longer than 10 min did not change the IR spectrum, revealing that the photocyclization was completed within 10 min. The conversion was calculated based on the intensity change in the absorption at 1678 cm^{-1} to give the almost linear relationship with the irradiation time (Figure 4b).

The morphological changes of the microcrystals during the photocylization were observed by AFM. Figure 5b shows the AFM image of a piece of microcrystal before irradiation. The top surface is the (100) plane. In contrast to the bulk crystals, surprisingly, the microcrystal maintained the single-crystalline phase in the course of the photocyclization (Figure 5c,d). No cracks were recognized during and after the completion of reaction. The shape and the size of microcrystal were the same as the reactant crystal. We could not understand the reason for no change of the morphology because the crystal structures between the reactant (*S*)-**1** and the product (*R*,*S*)-**2** are different (Table 1).

Hence, powder X-ray diffraction profiles were recorded to elucidate the reaction process. When the reactant crystals of (*S*)-**1** were submitted to UV irradiation (Figure 6a), several new peaks appeared and oppositely the intensities of reactant peaks decreased (Figure 6b). It reveals that the photocyclization proceeds with accompanying the phase separation between the reactant crystals and the product crystals. The profiles changed continuously and irradiation for 500 min completed the reaction, giving the product (*R*,*S*)-**2** (Figure 6c). Interestingly, recrystallization of the product crystals from acetonitrile changed to the crystal structure (Figure 6d), which was completely co-incident with the diffraction profile from the X-ray crystallographic analysis using the single crystal (*R*,*S*)-**2** obtained by recrystallization from acetonitrile (Figure 6e).

The relatively resemblance of diffraction profiles between the reactant (Figure 6a) and the product (Figure 6c) suggests that the single-crystal-to-single-crystal reaction might occur. However, the photocyclization proceeds from the surface of single crystal by UV irradiation, and therefore, the strain is

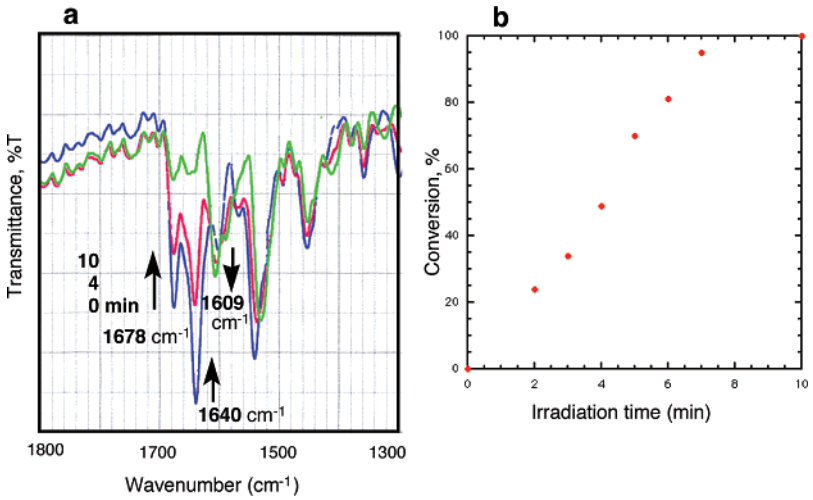

FIGURE 4. (a) IR spectral change and (b) conversion of the photocyclization of (*S*)-**1** in the microcrystals under UV irradiation.

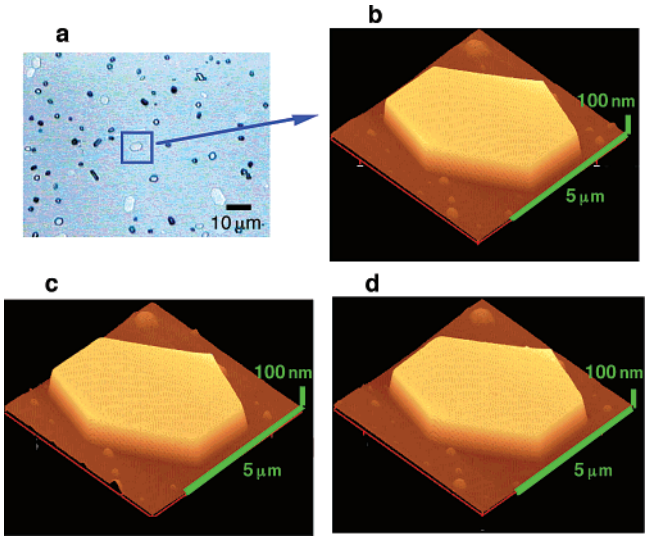

FIGURE 5. Microcrystals of (*S*)-**1** and the AFM images of the morphological change under UV irradiation: (a) and (b) before UV irradiation, (c) 50% conversion after 4 min, and (d) 100% conversion after 10 min.

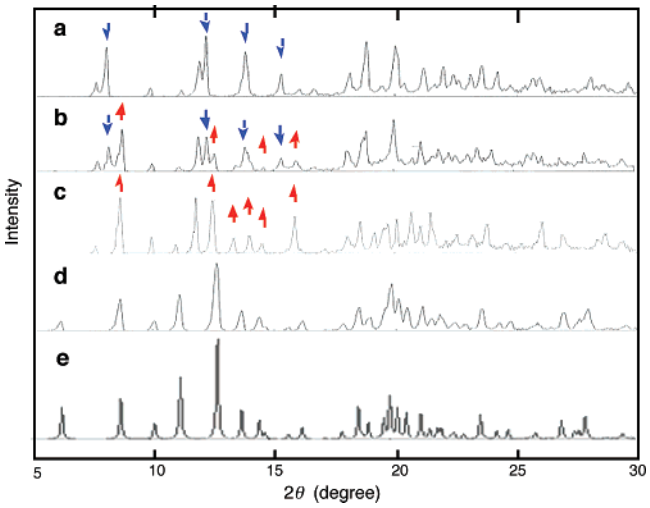

FIGURE 6. Powder X-ray diffraction profiles: (a) before irradiation of (*S*)-**1**, (b) after irradiation for 20 min, (c) product (*R*,*S*)-**2** obtained by irradiation for 500 min, (d) recrystallized (*R*,*S*)-**2**, and (e) profile from the X-ray crystallographic analysis of the recrystallized (*R*,*S*)-**2**.

generated within the crystal lattice to lead to crack and break into the polycrystals. On the other hand, the strain accumulated in the microcrystals is so small that the reaction can be completed in keeping the initial single-crystalline shape. Recently, Takahashi et al. reported that in the topochemical polymerization by successive [2 + 2] photocyclization of diolefin derivatives the bulk crystal was broken into fragments during polymerization but the nanocrystals maintained the single-crystalline phase in the course of polymerization.[17]

In conclusion, the diastereospecific photocyclization of (*S*)-**1** was found to proceed without any change of the morphology in the microcrystals, suggesting the single-crystal-to-single-crystal transformation, even the breaking of bulk crystals. X-ray crystallographic analysis of the product single crystal by careful UV irradiation of the reactant crystal is now underway. When complete, the results will be published elsewhere.

Experimental Section

Preparation of (*S*)-1. 2,4,6-Triisopropyl-2′-carboxybenzophenone (0.201 g, 0.57 mmol) and (*S*)-phenylethylamine (0.20 g, 1.8 mmol) were dissolved in chloroform (10 mL) and THF (1 mL) followed by addition of triethylamine (2.0 mL, 14 mmol) and BOP (0.50 g, 1.2 mmol). The solution was stirred at room temperature for 18 h, and the solvent was evaporated in vacuum. The crude product was purified via silica gel column chromatography (hexane/ethyl acetate, 10:1) to afford white powder (*S*)-**1** (0.232 g, 0.51 mmol, 90% yield). Characterization: mp (acetonitrile) 141.2−143.8 °C (uncorrected); ^{1}H NMR (300 MHz, $CDCl_3$, TMS) δ 1.10 (d, J = 6.30 Hz, 12H), 1.27 (d, J = 6.60 Hz, 6H), 1.69 (d, J = 6.60 Hz, 3H), 2.74 (septet, J = 6.60 Hz, 2H), 2.93 (septet, J = 6.60 Hz, 1H), 5.40−5.49 (m, 1H), 6.18 (d, J = 8.10 Hz, 1H), 7.05 (s, 2H), 7.27−7.56 (m, 9H); IR (KBr) 3279, 1680, 1640 cm^{-1}. Anal. Calcd for $C_{31}H_{37}NO_2$: C, 81.72; H, 8.18; N, 3.07. Found: C, 81.85; H, 8.22; N, 3.16.

Solid-State Photolysis of (*S*)-1. Pulverized crystals of (*S*)-**1** (0.200 g, 0.44 mmol) were placed between two Pyrex plates and irradiated with a 400 W high-pressure mercury lamp under argon at 20 °C for 8 h to give cyclobutenol (*R*,*S*)-**2** (0.200 g, 0.44 mmol, 100% yield) as the sole product. Characterization of (*R*,*S*)-**2**: white powder; mp (acetonitrile) 146.2−148.3 °C; ^{1}H NMR (300 MHz, $CDCl_3$, TMS) δ 0.75 (s, 3H), 1.22−1.26 (m, 9H), 1.29 (s, 3H), 1.33 (d, J = 7.02 Hz, 3H), 1.66 (d, J = 6.90 Hz, 3H), 2.88 (septet, J = 6.90 Hz, 1H), 3.03 (septet, J = 6.90 Hz, 1H), 5.26−5.38 (m, 1H), 6.32 (d, J = 7.20 Hz, 1H), 6.78 (s, 1H), 7.05 (s, 1H), 7.20−7.55 (m, 9H); IR (KBr) 3316, 1611 cm^{-1}. Anal. Calcd for $C_{31}H_{37}NO_2$: C, 81.72; H, 8.18; N, 3.07. Found: C, 81.76; H, 8.17; N, 3.18.

Solution Photolysis of (*S*)-1. A solution of (*S*)-**1** (2.51 g, 5.51 mmol) in acetonitrile (100 mL) was internally irradiated with a 100 W high-pressure mercury lamp at room temperature for 54 h under the bubbling of argon. The solvent was evaporated from the irradiated solution, and the residue was submitted to silica gel column chromatography (hexane/ethyl acetate, 10:1) to give (*R*,*S*)-**2** (0.60 g, 1.34 mmol, 24% yield) and (*S*,*S*)-**2** (0.536 g, 1.18 mmol, 21% yield) as diastereoisomeric products and remaining starting (*S*)-**1** (0.851 g, 1.87 mmol, 66% conversion). Characterization of (*S*,*S*)-**2**: white powder; mp (acetonitrile) 137.2−139.0 °C; ^{1}H NMR (300 MHz, $CDCl_3$) δ 0.98 (s, 3H), 1.22−1.30 (m, 9H), 1.33 (d, J = 6.90 Hz, 3H), 1.51 (s, 3H), 1.66 (d, J = 6.90 Hz, 3H), 2.90 (septet, J = 6.90 Hz, 1H), 3.07 (septet, J = 6.90 Hz, 1H), 5.31−5.42 (m, 1H), 6.30 (d, J = 7.80 Hz, 1H), 6.83 (s, 1H), 7.07 (s, 1H), 7.25−7.48 (m, 9H); IR (KBr) 3319, 1634 cm^{-1}. Anal. Calcd for $C_{31}H_{37}NO_2$: C, 81.72; H, 8.18; N, 3.07. Found: C, 81.77; H, 8.18; N, 3.13.

X-ray Crystallograhic Analysis. X-ray diffractions were collected on an imaging plate two-dimensional area detector using graphite-monochromatized Cu Kα radiation. All the crystallographic calculations were performed by using teXsan[18] or CrystalStructure crystallographic software.[19] The structure was solved by direct methods and expanded using Fourier techniques. The non-hydrogen atoms were refined anisotropically, and hydrogen atoms were not refined. Hydrogen atoms attached to carbon atoms were located in the calculated positions. Absolute structure was determined by the

(17) Takahashi, S.; Miura, H.; Okada, S.; Oikawa, H.; Nakanishi, H. *J. Am. Chem. Soc.* **2002**, *124*, 10944−10945.

(18) TeXsan, X-ray Structure Analysis Package, Molecular Structure Corporation, The Woodlands, TX, 1985.

(19) CrystalStructure, Ver. 3.7, Rigaku Corp., Tokyo, 2005.

S configuration of phenylethylamide group of the molecule. The crystal data are summarized in Table 1.

Acknowledgment. This work was supported by a Grant-in-Aid for Scientific Research (KAKENHI) in Priority Area "Molecular Nano Dynamics" from the Ministry of Education, Culture, Sports, Science and Technology of Japan and the Asahi Glass Foundation.

Supporting Information Available: Details for the general experimental methods and NMR spectral data and crystallographic information for (*S*)-**1**, (*R*,*S*)-**2**, and (*S*,*S*)-**2**. This material is available free of charge via the Internet at http://pubs.acs.org.

JO071005I